

Multi-wavelength imaging system for the Dutch Open Telescope

Felix C.M. Bettonvil^{*a,b}, Robert H. Hammerschlag^a, Peter Sütterlin^a,
Aswin P.L. Jägers^c, Robert J. Rutten^a

^aAstronomical Institute, Utrecht University, The Netherlands;

^bNetherlands Foundation for Research in Astronomy NFRA, Dwingeloo, The Netherlands;

^cPhysics Instrumental Group IGF, Utrecht University, The Netherlands

ABSTRACT

The Dutch Open Telescope (DOT) is an innovative solar telescope, completely open, on an open steel tower, without a vacuum system. The aim is long-duration high resolution imaging and in order to achieve this the DOT is equipped with a diffraction limited imaging system in combination with a data acquisition system designed for use with the speckle masking reconstruction technique for removing atmospheric aberrations.

Currently the DOT is being equipped with a multi-wavelength system forming a high-resolution tomographic imager of magnetic fine structure, topology and dynamics in the photosphere and low- and high chromosphere. Finally the system will contain 6 channels: G-band (430.5 nm), Ca II H (K) (396.8 nm), H α (656.3 nm), Ba II (455.4 nm), and two continuum channels (432 and 651 nm).

Two channels are in full operation now and observations show that the DOT produces real diffraction limited movies (with 0.2'' resolution) over hours in G-band (430.5 nm) and continuum (432 nm).

Keywords: diffraction limited imaging, solar telescopes, telescope optics, speckle masking technique, seeing, stray light, magnetic structure

1. DUTCH OPEN TELESCOPE

1.1 Introduction

The Dutch Open Telescope (DOT) at the Roque de los Muchachos Observatory at La Palma (Figure 1) uses the wind for minimizing telescope seeing. Both telescope and tower are open, without use of a vacuum system. It was proposed by C. Zwaan during the JOSO-LEST test campaigns in the 1970's -based on measurements showing reasonable better seeing conditions 10-30 m above ground surface¹- and designed by R.H. Hammerschlag. When the wind blows sufficiently strong it confines the solar-heated boundary layer of turbulent convection to heights below the telescope and flushes the telescope itself. On the excellent location of La Palma (2350 m) best seeing occurs when the wind is coming from northern direction (trade winds), bringing stable and undisturbed air to the telescope. Figure 2 shows an example of a (G-band) image, taken with the DOT. More images and movies can be found on the DOT website: <http://dot.astro.uu.nl>.

The telescope construction is simple and easily up-sizeable towards (much) larger apertures, introducing a new class of high-resolution solar telescopes.

1.2 Mechanical construction

For the whole telescope construction counts that every piece needs to be extraordinarily stiff to avoid image shake from wind buffeting and needs to be transparent as well for not disturbing the wind profile. The support tower has a height of 15 m and is constructed with parallel triangles, in two pairs and perpendicular to each other. Each pair gives stiffness in one direction and parallel guidance in the perpendicular direction. In this way the platform is always kept parallel, avoiding rotations rather than translations. Rotation and tilt introduce motion in the telescope image, translation is harmless (because the sun is at infinity). Interferometric measurements during tests in the Netherlands showed that the tilt of the platform at wind gusts up to 10 m/s is not more than 0.1''².

^a F.C.M.Bettonvil@astro.uu.nl; phone +31 30 2535218/2535200; fax +31 30 2535201; <http://dot.astro.uu.nl>; Astronomical Institute, Utrecht University, Princetonplein 5, 3584 CC Utrecht, The Netherlands

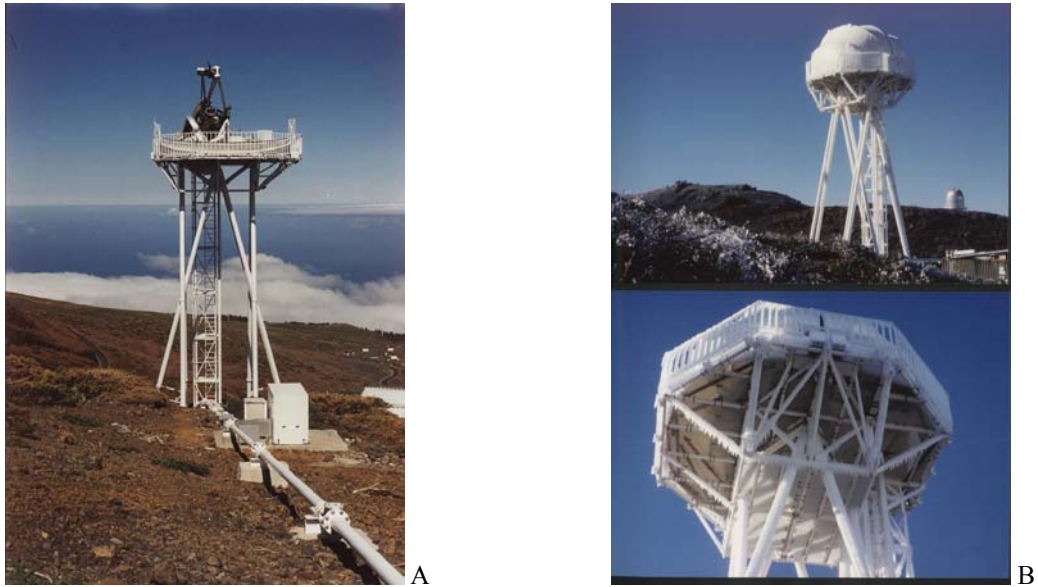


Fig. 1: The Dutch Open Telescope on La Palma: a) open and pointed to the sun (photo Aswin Jägers); b) closed with ice on the steel construction on a winter day (photo Rob Hammerschlag).

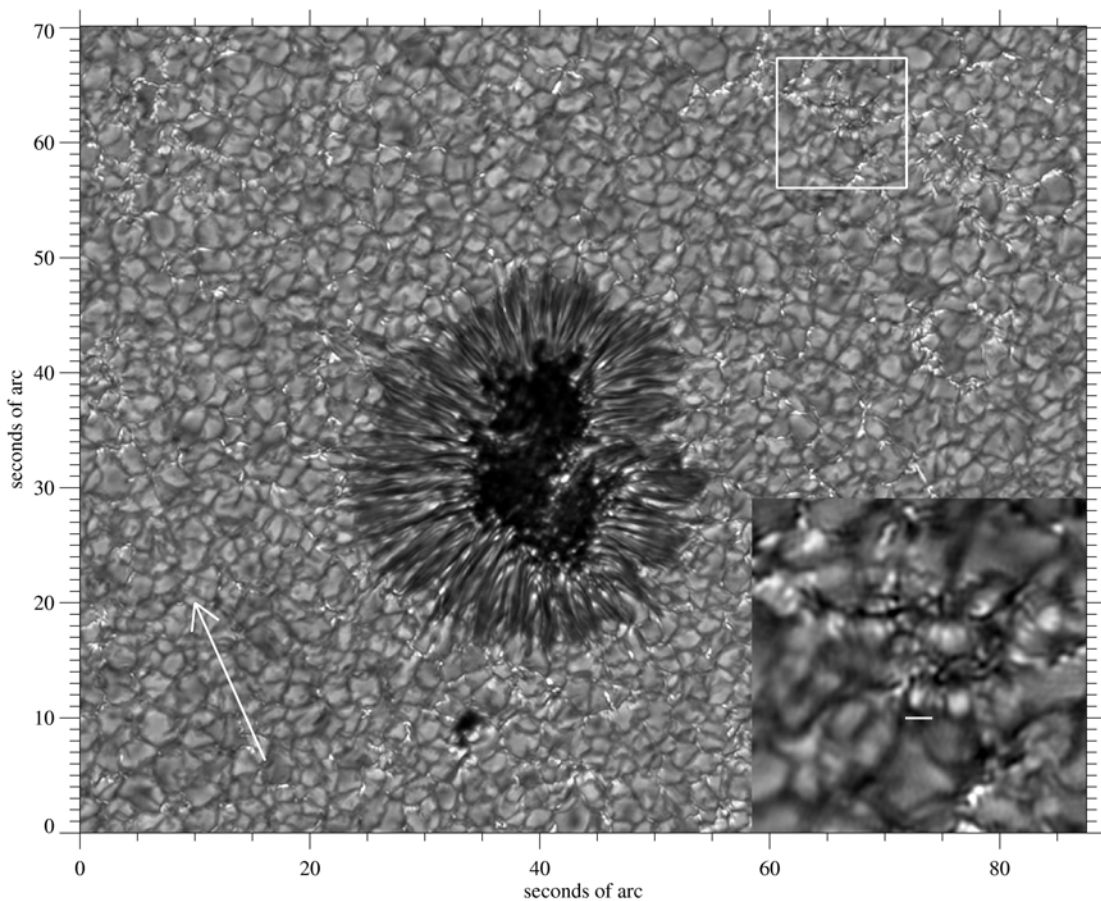


Fig. 2: Example of a DOT G-band image: AR 9407 taken on April 1, 2001 (Peter Sütterlin). The white bar in the cutout equals $1''$. The white arrow directs towards disk center. The image is a single frame from a 1-hour movie, available on <http://dot.astro.uu.nl>.

To minimize wind shake the whole platform and telescope construction is kept as small as possible and symmetrical (minimizing torque) and the staircase is completely decoupled from the tower during observations. The different legs of the tower have slightly different eigen-frequencies and are halfway connected with a damping element to avoid excitation by wind. So far, high-resolution solar observations are done with wind speeds above 20 m/s and no vibrations by wind have been observed. Details about the tower are given in ^{2,3}.

The mount of the telescope is of the equatorial fork type (Figure 3a). The choice of an equatorial mount has the advantage not having any time-varying polarization effects inside the optical system, and no need for an image rotator. The mount is fully exposed to wind too and built compactly to maximize stiffness. Unusual is that the telescope itself is mounted in the fork unbalanced: the primary mirror is located in front of the declination axis, in order to put the optical light path as much as possible in the free wind flow. Consequently a short fork construction can be used, increasing stiffness⁴.

Both hour angle axis and declination axis contain 2 motors. The teeth are relatively large for a telescope like the DOT, but have been chosen for maximum stiffness. In a gear system, stiffness is only obtained when two neighboring teeth do have contact over the full width of a tooth, so-called line contact. Consequently the alignment takes extreme care because flexibility in the tooth is minimal with the relatively small forces applied on a telescope. The DOT gear trains (Figure 3b) do have a novel self-aligning mechanism to ensure that all neighboring teeth have line contact⁵. Care has been taken to minimize the force on every tooth to prevent the stick-slip effect, which introduces a non-smooth movement, caused by a combination of flexibility, load and non-linear friction behavior at very low speeds. Tests in the workshop showed a reproducibility of 2 μm at the top of the telescope (located 2.5m away from the rotation axis).

One of the motors of each axis is driving the gears, the other is delivering a minimal and adjustable preload, avoiding backlash. Every day around noon the function of both motors is exchanged due the change of the center of gravity of the telescope from east to west, reversing the preload.

The motors are of the brushless servo type and connected to a home built motor-controller. A guider system, based on the image of a small auxiliary telescope, computes the center of the solar disk every 0.1 seconds and sends corrections to the motor controller.

The telescope construction, supporting the optical system, is like the tower built based on triangles too and looks unlike the slim looking tower heavy. For precise alignment of the optical components both translations and rotations need to be minimized. The base of the construction is large enough to accommodate much larger mirrors than the 45 cm mirror at present (Figure 3c).

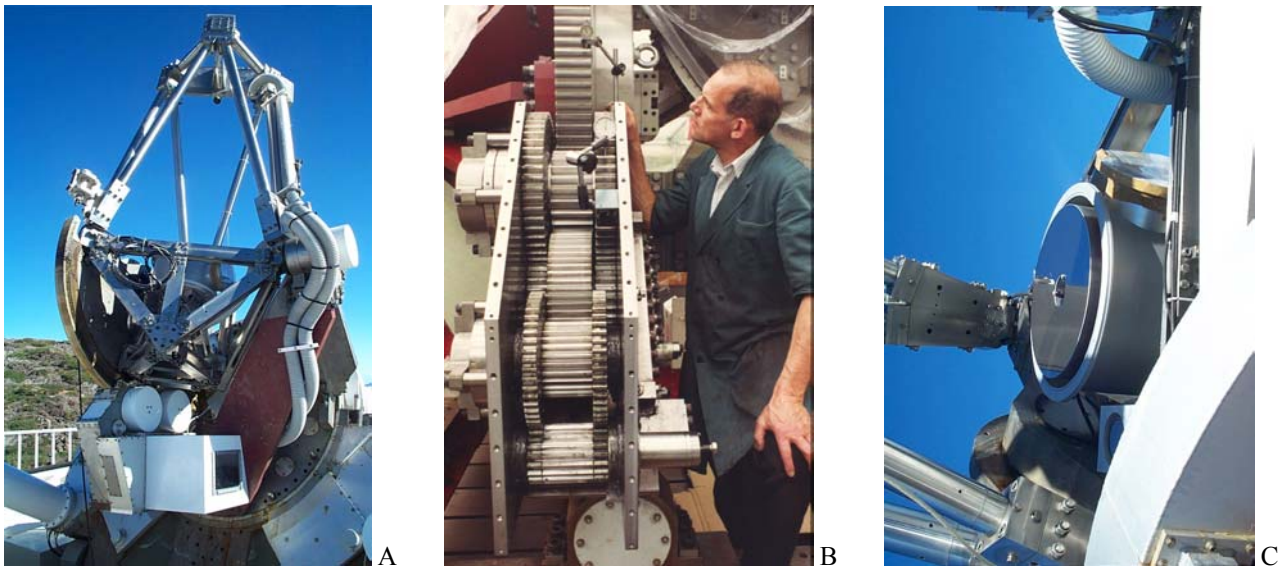


Fig. 3: a) Close up of the telescope with mirror cell, suction hoses and gear system ; b) interior of the gear system during assembling with DOT technician Piet Hoogendoorn; c) detail of the mirror cell with 45-cm mirror (photos Rob Hammerschlag).

A 7-m clamshell foldaway tent protects the telescope from (sometimes very) inclement weather. During observations the tent can be opened completely with very little obstruction to the wind left (see Figure 1), being essential for the DOT open principle. It consists of rotatable steel bows with in between tent cloth made of PVC coated with a teflon-like material (PVDF). When closed the cloth is spanned around the bows and the unique saddle form of the cloth guarantees survival during severe weather conditions. The floor of the tent is made of grating and only closed with wooden panels in winter.

The tent can be opened and closed until 30 m/s and is designed to withstand wind gusts up to 70 m/s. The coated fabric also tends to resist ice deposition, otherwise a major problem on the La Palma summits where undercooled fog often cause icicle growth. A larger version of the DOT enclosure is now being designed for the new German GREGOR telescope⁶.

1.3 Optical system

The original DOT optical system (Figure 4) is fairly simple and consists of a 450 mm/F4.44 parabolic mirror and a 10x-enlargement lens system directly behind the prime focus inside the primary beam, called secondary optics system. The use of the DOT is without adaptive optics, and uses the speckle reconstruction technique (see next section) for image restoration.

The mirror is made of Cervit with aluminum coating and quartz protection coating. The outer 19 mm and worst part of the mirror is not used, and covered by a stop in the pupil plane as imaged by the secondary optics. The primary mirror and secondary optics are carefully aligned to ensure the real optical axis of the primary mirror coincides with the secondary optics within 0.1 mm. To achieve this the primary has been measured interferometrically before assembling, and the aberration free area marked with a stiff mechanical cone and laserdiode too for redundancy.

The image size of the solar disk in the prime focus is 18 mm. A field stop (Figure 5 and 6), 50 mm in diameter, contains a central hole of 1.6 mm diameter, and blocks most of the light, preventing heat load and stray light entering the secondary optics, and limits the field to 3'. On the field stop in total 200 W of heat power is concentrated and needs to be prevented leaking into the surrounding air inside the telescope beam. For this reason the field stop is made of high conductive copper, containing a labyrinth of canals, extending to 1 mm below the surface (to minimize temperature differences between exposed and non-exposed areas on the surface) through which water is pumped of ambient temperature at a flow rate of 6 l/min. The cooling circuit is passive; cooling water is stored in a 300 liter (see white box in Figure 1) water tank located (together with pump) 30 m away from the telescope and pumped around.

The front surface of the field stop is 15° tilted and polished and coated with protected silver, reflecting most of the heat outside the telescope. Around the field stop an additional cylinder has been designed to suck away all air surrounding the field stop.

Provisions are made to flush the primary mirror too, possibly giving an additional improvement in seeing at lower wind speeds, but not yet installed. Critical directly exposed parts of the telescope are made white, using a paint containing TiO₂ pigment.

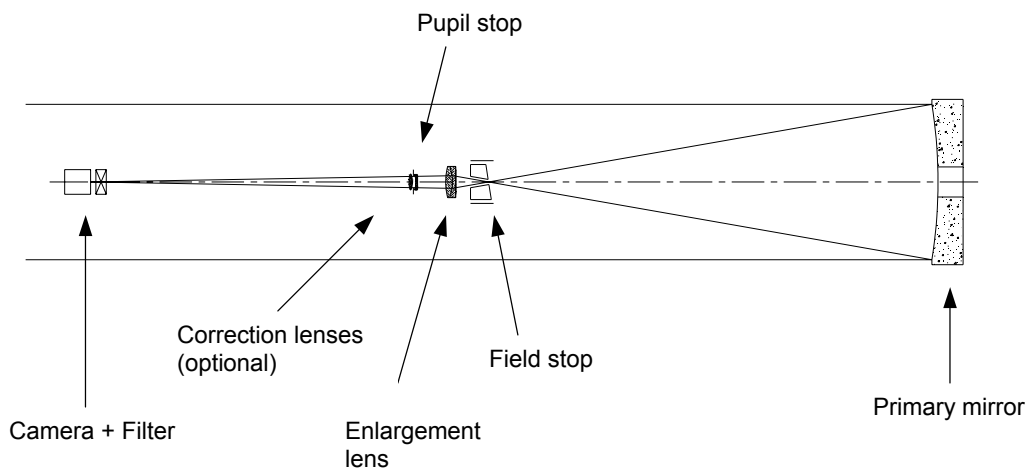


Fig. 4: Scheme of the optical system with field stop and secondary optics.



Fig. 5: Field stop mounted on the front side of the secondary optics. The surface is coated with protected silver. In the center the hole with 1.6 mm diameter is visible.

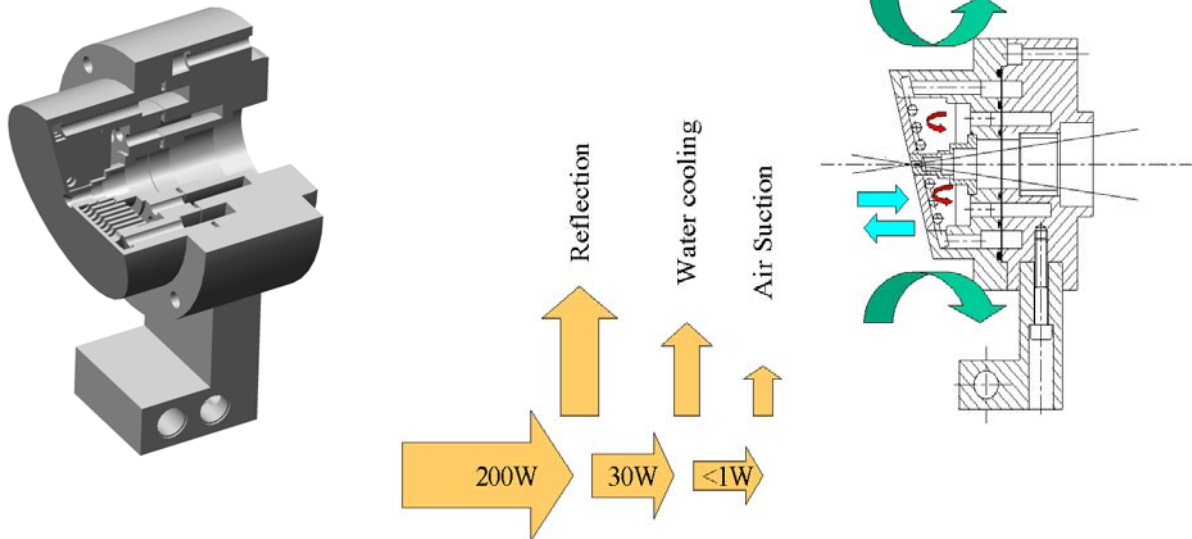


Fig. 6: a) Cut away view of the water-cooled field stop, b) heat budget.

The secondary lens system, located after the field stop, is designed to magnify the primary image 10x, fitting the spatial resolution limit ($0.2''@430\text{nm}$) to the pixel size of the camera ($6.7 \times 6.7 \mu\text{m}^2$). The enlargement system consists of two cemented doublets. The first doublet -available off the shelf and carefully selected- is located just 60 mm after the field stop and is the most exposed lens in the system. Lab measurements didn't show any deteriorating of the image quality under heat load. The second doublet has been designed ourselves and corrects for coma and spherical aberration at 430 nm. The lens system corrects for the coma caused by the parabolic mirror too increasing the usable field size to the maximum 3° .

The lens system still suffers from sphero-chromatism, the change of spherical aberration with wavelength. The wavelength with minimum spherical aberration can be 'tuned' by use of an extra pair of two lenses located nearby the pupil with a negligible power (see Section 3.1). Close to the lens system the pupil is imaged and a stop functions as the main stray light prevention. At the end of the lens system only an interference filter (usually G-band, 430.5 nm, 1 nm FWHM) and camera are located. The optical path is only approximately telecentric.

Focussing and flat fielding is done by moving the whole secondary optics including field stop and camera relative to the primary mirror.

1.4 Speckle restoration

The Speckle Masking Method^{7,8,9,10,11,12} is generally used for restoring solar observations on the DOT¹³. This sets the DOT apart from the atmospheric restoration programs elsewhere which rely on adaptive optics. It uses the fact that short-exposure images freeze the atmospheric distortions while still showing signal at high spatial frequencies, although with statistically disturbed phases. Speckle reconstruction through the Speckle Masking technique is a well-established technique also in solar physics but never applied on a scale which the DOT will employ it.

The speckle technique only corrects for statistical disturbances caused by the earth atmosphere, hence all systematic errors, i.e., optical aberrations, do still degrade the image quality after reconstruction. For this reason the optical system needs to be of excellent quality to obtain images and movies showing details at the resolution limit of the telescope. In particular residual optical aberrations do degrade the highest spatial frequencies, while a central obstruction mainly influences the middle range¹⁴.

Figure 2 shows a sample G-band image. It illustrates the high-resolution achieved with the DOT and it also illustrates the important advantage the speckle processing has over adaptive optics: the whole field as delimited by the CCD restored to the 0.2'' diffraction limit, due to the fact that the full image is splitted into hundreds of iso-planatic patches, treated indepently, contrary to adaptive optics which fully corrects strictly only for one patch. This quality is reached whenever the seeing is moderately good, i.e., Friedparameter $r_0 \approx 10$ cm. On La Palma this is frequently the case and holding for long periods, resulting in the typical DOT-movies as downloadable from <http://dot.astro.uu.nl>.

In the speckle observing mode, for every reconstructed image about 100-200 images (depending on seeing) are taken within a time scale that the solar scene doesn't change (15-30 s) with exposure times not more than 10 ms to 'freeze' the seeing. The needed short exposure time makes that speckle is not well suited for feeding spectrometer slits.

2. DOT SCIENCE

The science niche that the DOT may fill the coming years consists of delivering long-duration image sequences that excel in angular resolution, field size, multi-height sampling and diagnostic value. These properties make the DOT a tomographic mapper of the time-dependent magnetic topology of the solar atmosphere at intrinsically different heights, useful and desirable to all issues in which magnetic topology plays a role – ranging in spatial scale from tiny network flux tubes to extended active regions, in temporal scale from high-frequency oscillations to active-region evolution, in dynamical behavior from stable (but oscillating) sunspots to flares, erupting prominences, and coronal mass ejections, in pattern topology from ephemeral field emergence and network field dispersal to the structure and evolution of active regions and the anchor constraints to filament/prominences and flare build-up.

Table 1 shows the wavelengths of interest. The G-band contains many dark CH lines, which vanish through CH dissociation in magnetic elements, making this band the best diagnostic to map 'flux tubes' in the deep photosphere. The Ca II H (K) line shows the magnetic field distribution higher up where the magnetic elements combine into larger network patches but the field has not been spread all over. The field spreading into finely textured and highly dynamic magnetic 'canopies' is seen in H α . The Ba II resonance line has enhanced Doppler sensitivity to non-thermal motions at high angular resolution due to the large atomic mass of barium and may also be a good Stokes line.

The DOT science goal is to provide a link between ground-based high-resolution mapping of the magnetic topology of the solar photosphere and chromosphere and space-based short-wavelength imaging with missions as TRACE and SOHO which sample the transition region and corona.

Diagnostic	λ [nm]	$\Delta\lambda$ [nm]	domain
G band	430.5	1	low photosphere
Ca II H	396.8	0.1	low chromosphere
H α	656.3	0.025	high chromosphere
Ba II	455.4	0.008	low photosphere

Table 1: Selected wavelengths for the DOT multi-wavelength system.

3. MULTI-WAVELENGTH IMAGING SYSTEM

3.1 Optical setup

For upgrade from one channel towards a multi-channel system containing cameras imaging in G-band, Ca II H (K)-, H α - and Ba II as mentioned in table 1, the top area of the telescope has been selected. The top structure is stiff enough to support a few hundred kilograms of instrumentation and the area is not space limited. Figure 7 illustrates the extension schematically, Figure 8 the actual design. In addition to the 4 mentioned channels 2 extra have been added, a continuum channel at 432 nm and a continuum channel nearby H α . The latter is needed to enable tuned narrow-band speckle restoration of the H α line using the two-channel technique of Keller & von der Lüh⁷. Chosen is for a lens system based on experiences with the original secondary optics. An alternative all-mirror scheme using a second parabolic mirror has been regarded, being more complex mechanical, but is a reasonable alternative when using larger apertures³.

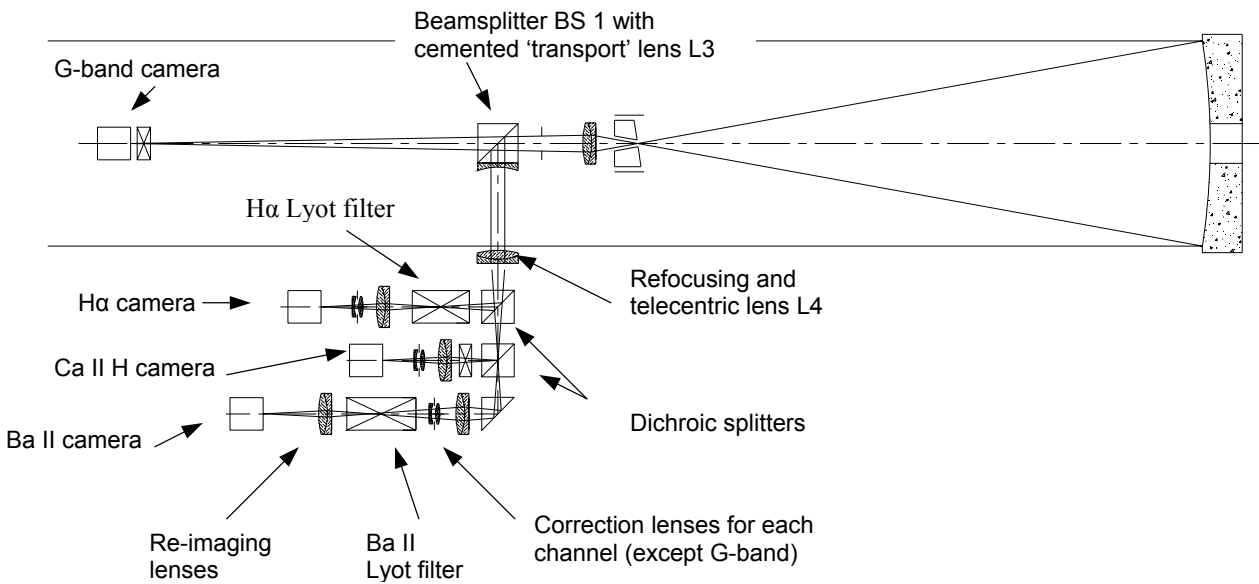


Fig. 7: Optics sketch of the upgrade from the secondary optics (see Figure 4) towards a multi-wavelength imaging system. For clarity the two continuum channels have been neglected and the splitting optics simplified: in reality the splitters are not cubes but mirrors reflecting on a small angle.

High-resolution observing, even on the Sun, is always short on photons. With 0.07'' pixelsize, 10 ms exposure time and 0.025 nm bandwidth for H α only a few thousand photons are collected, so that much care must be taken not to be drowned in noise. Wherever possible dichroic splitters and polarizing splitters are used.

All new channels are fed from a broadband beamsplitter cube BS1 (Figure 7 and 8) located inside the original secondary optical system (but fixed to the main structure and not to the secondary optical system, which is movable for focussing): 10% is transmitted towards the G-band, 80% reflected towards the new channels. On BS1 a negative doublet L3 has been cemented to transport the beam outside the telescope and refocused by another (now positive) doublet L4. This lens has a second purpose, it acts as a telecentric lens too, delivering a pupil image at infinity for all new channels.

Splitting between H α and Ca II H/ Ba II/ blue continuum is done by a dichroic mirror BS2 (transmitting 600-700 nm and reflecting 380-460 nm) slightly tilted (8°) to minimize the introduction of astigmatism. Splitting between Ca II H and Ba II/ blue continuum is done with a second dichroic mirror BS3 (transmitting 415-460 nm, reflecting 380-400 nm), and tilted at the same angle.

Distribution of the light between the H α line and H α continuum is not done by use of dichroic mirrors because the wavelength bands are too close, but with a polarizing beam splitter, to direct as much as possible to the (polarization sensitive) Lyot filter. A polarizing splitter is used too for distribution between Ba II and blue continuum.

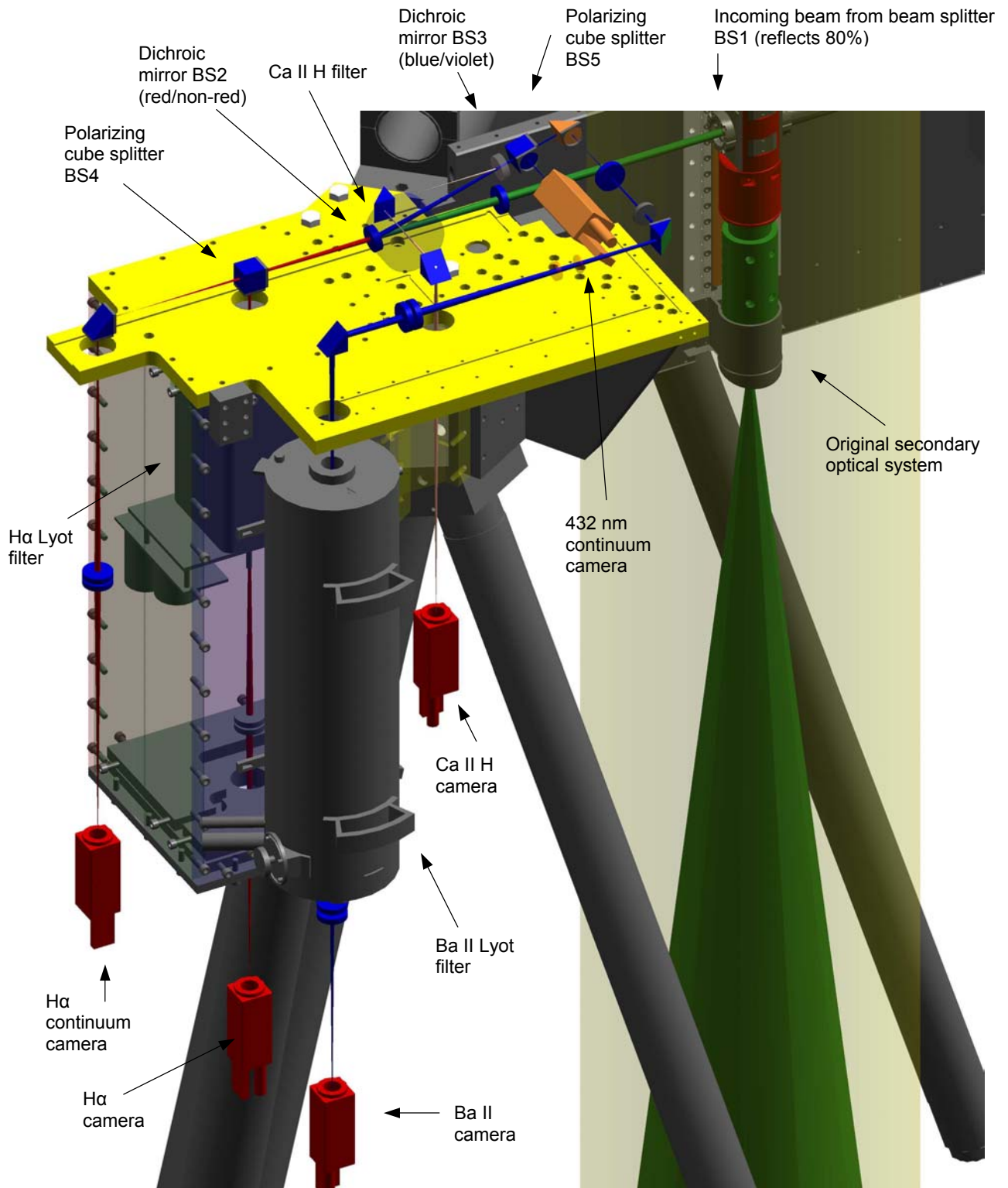


Fig. 8: 3-dimensional overview of the complete multi-wavelength system with all covers removed. The G-band camera is situated at the back of the original secondary optical system and not visible (drawing Aswin Jägers).

Ca II H and H α need re-imaging lenses to be able to accommodate the filters, but are placed after the filters not influencing the telecentric perspective. All re-imaging lenses are long focal length lenses and do not add aberrations. The re-imaging lenses do create an extra pupil image too, and this location is effectively used to accommodate a pair of correction lenses. The shape of the correction lens greatly vary coma and spherical aberration without influencing other aberrations¹⁵ and this is used to shift the minimum spherical aberration towards the wavelength of observation as shown Figure 9.

The Ba II channel has the most complicated optical setup and needed a second pair of re-imaging lenses because of mechanical constraints. New in this design –compared to the other channels- is putting the correction lenses before the filter instead of behind it. This increases the freedom of optical magnification. In this perspective a compact zoomable optical system has been designed and is planned for the near future.

To reduce costs, off the shelf lenses have been used wherever possible. Custom lenses have only been manufactured for the correction lenses (tuning spherical aberration) and the transport lenses L3 and L4. For every lens the best piece from a small sample has been selected based on interferometric measurements. From this measurements we concluded that it is wise to use lenses with (much) larger diameters then strictly needed: the inner part of a lens has generally a reasonable better quality than the outer part. With help of an interferometer we designed lens mounts with tiny compression springs to minimize the stress on the lens, not degrading the optical quality and being stable too.

All applied filters are interference filters, except the H α and Ba II filters, which are both tunable Lyot filters (H α , tunable Zeiss formerly used at the Ottawa River Solar Observatory by V. Gaizauskas; Ba II built by V. Skomorovsky at Irkutsk). Both filters will be motorized for line profile scanning. For H α we think about 5-7 samplings across the line, being able to distinguish between brightness and Dopplershift modulation. For Ba II Dopplergrams will be produced. (First tests on the former SVST do look very promising as described by Sütterlin¹³.)

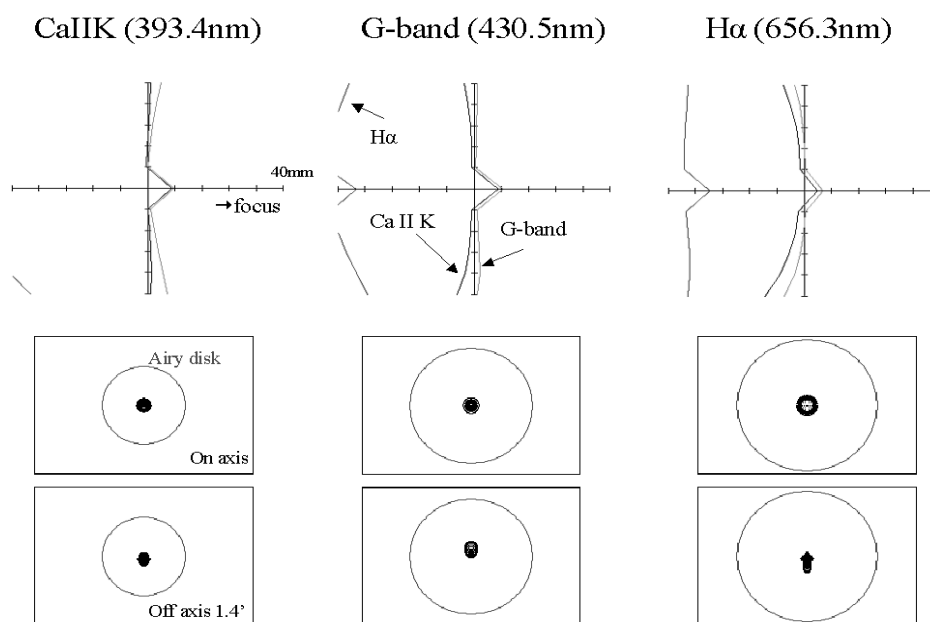


Fig. 9: Longitudinal aberration plots and spot diagrams for Ca II K, G-band and H α , after ‘tuning’ with the special correction lenses in each channel. Clearly is visible that only for one wavelength the spherical aberration is minimal.

The whole multi-wavelength system will be covered in boxes, preventing from straylight coming in and keeping the optics clean, and protecting against severe weather conditions. Every camera is mounted on micro-XY-stages for aligning all camera fields accurate. This exact alignment between all channels is important -and easily achievable due to the exceptional mechanical stability of the whole DOT- for employing H α as a principal canopy diagnostic delivering

insight in photosphere-corona magnetic coupling. DOT's Ca II channel can provide exact co-registration with TRACE UV images because their solar scenes correspond closely¹⁶. Stray light protection is done with baffles made of dry and coarse sandblasted and black anodized aluminum.

In July 2002, two channels are in full operation (Figure 12). Figure 11 shows an example of synchronously taken images in G-band (430.5 nm) and blue continuum (432 nm).

3.2 Focussing

One very important systematic error is defocus, which in fact is an optical aberration, but contrary to other optical aberrations not static but time-varying, mainly due to thermal expansion of the telescope structure. Defocus is very difficult to detect in the –by seeing disturbed- raw images, however clearly visible after speckle restoration and must be minimized. The focus tolerance is in the order of 0.01 mm in the primary focus of the telescope, about a tenth of the total focal shift during a whole observation day.

To compensate for defocus, an (auto) focus system, using an extra CCD-camera, has been designed based on the idea of comparing the contrast of an intra- and extra-focal image of some solar scenery. With the system the focus can be adjusted until both images show equal contrast. This position is by calibration the focus position of all cameras. To cancel out the effects of seeing, two images of exactly the same scenery are imaged on one CCD using an optical system that introduces a focus shift for one beam relative to the other, as shown in Figure 10.

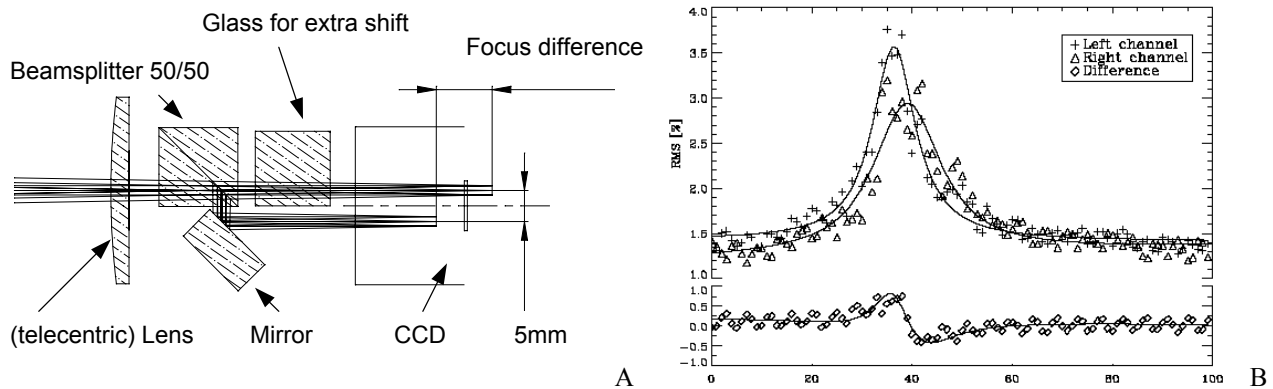


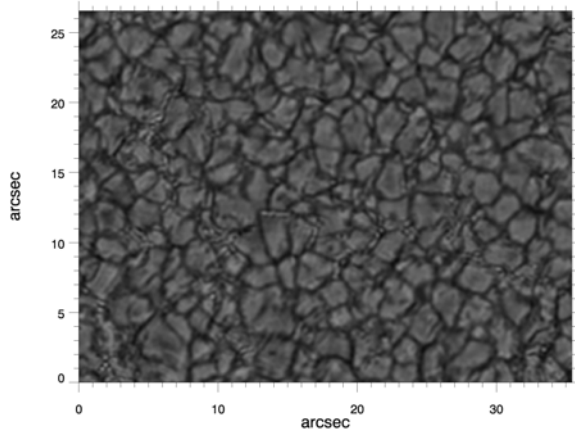
Fig. 10: a) Detail of the splitter optics, as used in the focus system. By use of a beam splitter an image of some solar scenery is splitted in two identical parts. The straight beam is imaged on the upper part of the CCD, the deflected beam on the lower part. Due to path difference of the deflected beam, as well as the additional glass put in the straight beam, the two images do have a focus difference at the CCD plane. b) Rms of the upper – (crosses) and lower image as a function of defocus (1 unit = 0.02 mm in primary focus). Seeing causes the fluctuations. The difference of the rms-values is a measure for the distance from focus and shown in the lower graph.

3.3 Data-acquisition

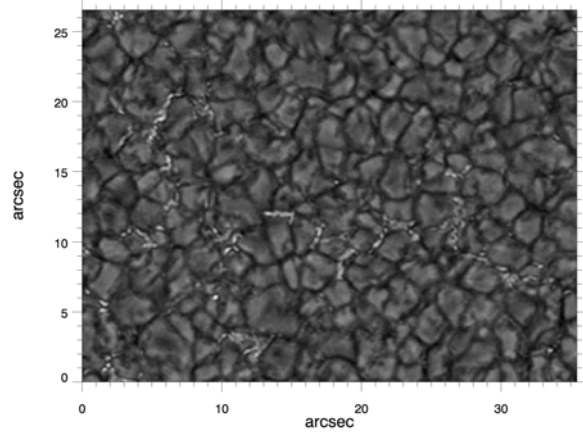
The data acquisition system collects consistently solar images in the form of synchronous speckle bursts using digital cameras. All channels are equipped with equal Hitachi KP-F100 camera's (1296x1030 pixels, size 6.7 μ m square, Sony ICX085 CCD, field size 92x73", 10 bit, max. 12 frames/sec). In fact the KP-F100 is a machine-vision camera and a compromise between speed, dynamic range, number of pixels, sensitivity in the blue and affordability.

Data transmission is done via 400 Mbps optical fiber links to the control room in the nearby New Swedish Solar Telescope (NSST), 100m away. The cameras are always run in synchronous speckle mode, each camera delivering 100-200 frames (called a burst), temporally stored in RAM and immediately after the burst stored on 72 Gb RAID disk arrays, totaling up to 350 Gb for all cameras per observing run (up to 2.5 hours at 30s burst cadence). Archiving is done during night on high-density tape cartridges (Exabyte Mammoth-2 robot containing 7 cartridges). Each camera has its own acquisition PC (Compaq Proliant ML-350 with IPC digital framegrabber) and all are controlled from a central workstation. When not in use for observations and backing up the computers are in use for image restoration.

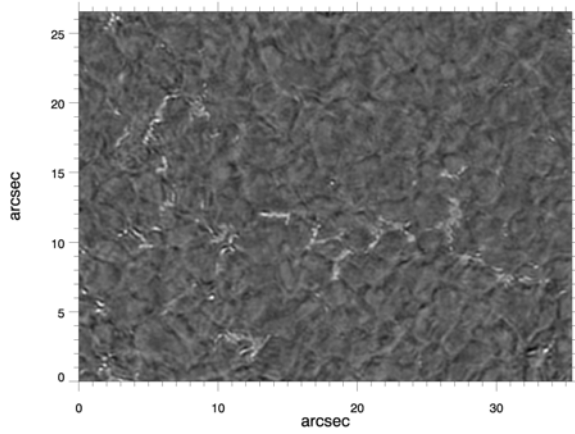
The whole acquisition system, including the fiber links, has been designed and built by the Physics Instrumental Group of Utrecht University.



A



B



C

Fig. 11: Example of synchronous DOT imaging with the first two channels operational: a) continuum (432 nm), b) synchronous G-band (430.5 nm); c) “magnetic image” isolating the magnetic elements in the intergranular lanes through an algebraic combination of the two images. The images are small cutouts from a 100-minute 63x73” observation on October 19, 2001 by Alfred de Wijn. The whole movie is in mpeg available at <http://dot.astro.uu.nl>.



A



B

Fig. 12: a) Image acquisition system; b) top of the telescope with secondary optics (central tube), continuum camera (box below) and focus system (upper box).

4. FUTURE

The DOT data production rate is presently limited to only a few observing campaigns per year. They suffice for the Utrecht need, but severely underexploit the enormous DOT science potential. The main bottleneck is the very time consuming speckle processing, taking multiple months per observing day at present. Massive processor parallelization can speed it up to overnight turnaround. Overnight processing will permit us to open the DOT as a high-throughput facility available for solar high-resolution observing to the whole international community¹⁷.

The success of the DOT in obtaining superb image sequences has demonstrated the validity of the open concept. This demonstration and the availability of adaptive optics opens the way to much larger open solar telescopes, as the German GREGOR⁵ and the US ATST¹⁸. Vacuum systems are limited to about 1-m diameter due to the entrance window, the open DOT concept is in principle unlimited in size. In a way this counts for the DOT itself too, being not just a 45-cm class telescope, but is designed to accommodate much larger mirrors, up to 1.4-m diameter.

ADKNOWLEDGEMENTS

The DOT is operated by Utrecht University at the Spanish Observatorio del Roque de los Muchachos of the Instituto de Astrofísica de Canarias under agreement with the latter and is presently funded by Utrecht University, the Netherlands Graduate School for Astronomy NOVA, the Netherlands Organization for Scientific Research NWO, and SOZOU. The DOT has been built by the Physics Instrumental Group of Utrecht University IGF and the Central Workshop of Delft University (now DTO TU Delft) with funding from Technology Foundation STW. The speckle development was part of the EC-TMR European Solar Magnetometry Network ESMN. The DOT team enjoys hospitality at the solar telescope building of the Royal Swedish Academy of Sciences.

REFERENCES

1. P.N. Brandt, A. Righini, *The JOSO Site Testing Campaign: Techniques, Results and General Considerations*, LEST Technical Report No. 11, Institute of Theoretical Astrophysics, University of Oslo, Oslo, 1985.
2. R.H. Hammerschlag, "Excursion: Tower, Parking Lot, Geostationary Orbit", *Solar Instrumentation: What's next?*, R.B. Dunn, pp. 583-599, Sacramento Peak National Observatory, Sunspot, 1981.
3. R.H. Hammerschlag, A.P.L. Jägers, F.C.M. Bettonvil, "Large Open Telescope: Size-upscaling from DOT to LOT", these proceedings.
4. R.H. Hammerschlag, "Construction Outlines of the Utrecht Open Solar Telescope", *Solar Instrumentation: What's next?*, R.B. Dunn, pp. 547-582, Sacramento Peak National Observatory, Sunspot, 1981.
5. R.H. Hammerschlag, "A telescope drive with emphasis on stability", *SPIE* Vol. 444, pp.138-146, 1983.
6. website GREGOR: <http://www.kis.uni-freiburg.de/GREGOR>.
7. C.U. Keller, O. von der Lüche, "Solar speckle interferometry", *A&A* **261**, pp. 321, 1992.
8. G.P. Weigelt, *Opt. Comm.*, "Modified astronomical speckle interferometry 'speckle masking'", **21**, 55, 1977.
9. G. Weigelt, B. Wirtzner, "Image reconstruction by the speckle-masking method", *Optics Lett.* **8**, 389, 1983.
10. C.R. de Boer, F. Kneer, "Speckle observations of abnormal solar granulation", *A&A* **264**, L24, 1992.
11. O. von der Lüche, *Solar Phys* **268**, 374, 1993.
12. C.R. de Boer, "Empirical speckle transfer function measurements from partial eclipse observations of the Sun", *A&AS* **114**, 387, 1995.
13. P. Sütterlin, R.H. Hammerschlag, F.C.M. Bettonvil, R.J. Rutten, V.I. Skomorovsky, G.N. Domyshev, "A multi-Channel Speckle Imaging System for the DOT", *Advanced Solar Polarimetry – Theory, Observation, and Instrumentation*, M. Sigwarth, Procs. 20th NSO/SP Summer Workshop, ASP Conf. Ser., in press, 2001.
14. H. Rutten, M. van Venrooij, *Telescope Optics, Evaluation and Design*, Willmann-Bell, Richmond, 1993.
15. W.J. Smith, *Modern Optical Engineering*, McGraw-Hill, New York, 1966.
16. R.J. Rutten, "DOT Strategies versus Orbiter Strategies", *Solar Encounter: the first Solar Orbiter workshop*, A. Wilson, pp. 357, Tenerife, ESA SP-493, 2001.
17. R.J. Rutten, A.G. de Wijn, P. Sütterlin, F.C.M. Bettonvil, R.H. Hammerschlag, "Opening the Dutch Open Telescope", *Magnetic Coupling of the Solar Atmosphere*, Procs. Euroconference/IAU Colloq. 188, ESA SP-505, in press.
18. website ATST: <http://www.sunspot.noao.edu/ATST>.